Article (refereed) - postprint

Woolway, R. Iestyn; Jones, Ian D.; Hamilton, David P.; Maberly, Stephen C.; Muraoka, Kohji; Read, Jordan S.; Smyth, Robyn L.; Winslow, Luke A. 2015.
Automated calculation of surface energy fluxes with high-frequency lake buoy data.

Contact CEH NORA team at
noraceh@ceh.ac.uk

Title

Automated calculation of surface energy fluxes with high-frequency lake buoy data

Authors

R. Iestyn Woolway[1, 2,*], Ian D. Jones[1], David P. Hamilton[3], Stephen C. Maberly[1],

Kohji Muraoka[3], Jordan S. Read[4], Robyn L. Smyth[5], Luke A. Winslow[4]

Affiliations

[1] Lake Ecosystems Group, Centre for Ecology & Hydrology, Lancaster Environment

Centre, Library Avenue, Bailrigg, Lancaster, LA1 4AP, UK.

[2] Environmental Change Research Centre, University College London, Gower Street,

London, WC1E 6BT, UK.

[3] Environmental Research Institute, University of Waikato, Private Bag 3105,

Hamilton 3240, New Zealand.

[4] U.S. Geological Survey Center for Integrated Data Analytics, Middleton, Wisconsin,

USA.

[5] Center for Environmental Policy, Bard College, Annandale-on-Hudson, NY, USA.

*Corresponding author: riwoolway@gmail.com

Tel: +44 (0)1524 595890

Abstract

Lake Heat Flux Analyzer is a program used for calculating the surface energy fluxes in lakes according to established literature methodologies. The program was developed in MATLAB for the rapid analysis of high-frequency data from instrumented lake buoys in support of the emerging field of aquatic sensor network science. To calculate the surface energy fluxes, the program requires a number of input variables, such as air and water temperature, relative humidity, wind speed, and short-wave radiation. Available outputs for Lake Heat Flux Analyzer include the surface fluxes of momentum, sensible heat and latent heat and their corresponding transfer coefficients, incoming and outgoing long-wave radiation. Lake Heat Flux Analyzer is open source and can be used to process data from multiple lakes rapidly. It provides a means of calculating the surface fluxes using a consistent method, thereby facilitating global comparisons of high-frequency data from lake buoys.

Keywords

Software; GLEON; Instrumented buoy; Heat flux; Sensor technology.

Software availability

Lake Heat Flux Analyzer is written in MATLAB and is free to download (https://github.com/GLEON/HeatFluxAnalyzer). Users without access to MATLAB can use the web interface (heatfluxanalyzer.gleon.org) which runs Lake Heat Flux Analyzer on a remote server based on user input files and allows users to download results after completion.

1. Introduction

The dynamic coupling between lake and atmosphere depends on the transfer of momentum, heat and material, at the air-water interface. The magnitude of these fluxes influences physical processes within lakes which, in turn, have a major impact on lake ecology (George and Taylor, 1995; Winder and Schindler, 2004). In order to understand the functioning of lakes it is therefore imperative to have a detailed understanding of how different atmospheric forcing can affect the system. This is particularly true in the context of climate change (DeStasio et al. 1996; Desai et al. 2009) where interactions between the atmosphere and a lake are one of the major causes of alterations to lake ecology and biogeochemical fluxes.

Along with the exchange of radiant energy, the water surface turbulent fluxes play an integral part in the functioning of a lake. These fluxes, for example, produce sub-surface currents (Strub and Powell, 1986), influence ice-cover break-up dates (Anderson et al. 1996), and alter the strength and duration of thermal stratification. By influencing thermal stratification and mixing, surface energy fluxes can affect light availability to phytoplankton (MacIntyre, 1993), the metabolic cycles of primary producers (Staehr et al. 2010), and the rate of gas exchange between the lake and the atmosphere (MacIntyre et al. 2010). Surface energy fluxes are also often treated as upper boundary conditions for physical lake models (e.g. Peeters et al. 2002) and can be used to estimate the overall heat budget of lakes (Wetzel and Likens, 1991).

Direct measurements of turbulent fluxes at the water surface are expensive. A large amount of research has therefore focussed on the derivation of appropriate methods to estimate these fluxes from relatively well known and frequently measured variables (e.g. Garratt, 1977; Large and Pond, 1982; Fairall et al. 1996). These bulk aerodynamic parameterizations, however, require the use of transfer coefficients. Numerous bulk transfer coefficient schemes exist, which vary in complexity and sophistication (Renfrew et al. 2002).

Simple approaches using constants or relationships with wind speed (e.g. Jones et al. 2005; Mackay et al. 2011; Vachon and Prairie, 2013) are easy to apply but have limited accuracy, while the technical complexity of the full calculations limits their usage.

Surface flux estimates are sensitive to the choice of algorithms used (Blanc, 1985; Zeng et al. 1998) especially when they have been developed for a limited range of wind speeds (e.g. Chang and Grossman, 1999). Despite recent efforts to develop these algorithms, no single method is consistently used to calculate the surface fluxes in lakes, and studies which compare different calculation approaches are uncommon. An additional source of uncertainty in comparing surface flux estimates across lakes results from comparing data measured at different heights above the water surface on different lakes. Standardization of methodology and cross-lake comparisons can be facilitated with easy-to-use and freely available software.

Recent advances in aquatic sensor technology have resulted in large numbers of instrumented lakes that have enabled multiple cross-site collaboration (e.g. Read et al. 2012; Solomon et al. 2013). Indeed, collaborative science in limnology on a global scale is fast becoming the norm (Hanson 2007). In order to translate this present-day 'flood' of environmental data into reproducible science, the use and creation of shared analytical tools is critical (Porter et al. 2012). In the following, we introduce a program called "Lake Heat Flux Analyzer" which can be used to calculate surface energy fluxes from lake buoy data according to established methodologies available in the literature. We demonstrate the use of this program by calculating the surface energy fluxes for three lake datasets from the Global Lake Ecological Observatory Network (GLEON; http://www.gleon.org/).

2. Materials and methods

2.1. Site description

High-frequency observations of water temperature and meteorological drivers were collected from three lakes that range in surface area from 1.0 to 79.8 km^2. The study sites include one lake from the United Kingdom (Esthwaite Water), one lake from the United States of America (Lake Mendota) and one lake from New Zealand (Rotorua). Each lake is exposed to a temperate climate. They are seasonally stratified and none of the data series included occasions when the lakes were ice covered.

Surface water temperature and meteorological measurements from each lake were collected by several instruments and maintained by different organizations. Esthwaite Water is part of the United Kingdom Lake Ecological Observatory Network (UKLEON) and is maintained by the Centre for Ecology & Hydrology, United Kingdom. Air temperature and relative humidity were measured at a height of 2.14 m above the lake surface and wind speed was measured at a height of 2.85 m. The instrumented buoy on Lake Mendota is maintained by the North Temperate Lakes − Long Term Ecological Research (NTL-LTER) program, which includes lakes in northern and southern regions in the state of Wisconsin. Data were collected every minute and fifteen-minute averages were then computed from the high-frequency data. Air temperature, relative humidity and wind speed were measured at a height of 2 m above the lake surface. For Lake Mendota, hourly estimates of incoming long-wave radiation data were calculated from 15 minute values observed at the nearby, Madison National Oceanic & Atmospheric Administration radiation monitoring site. The monitoring buoy in Rotorua is maintained by the Lake Ecosystem Restoration New Zealand (LERNZ) program which aims to restore indigenous biodiversity in New Zealand lakes. High-resolution temperature and meteorological data from Rotorua were measured at fifteen-minute intervals from July 2007 to July 2008. Air temperature, relative humidity and wind

speed measurements were measured at a height of 1.5 m. Short-wave radiation was measured on each of the three lakes. Unlike the other meteorological variables measured, short-wave radiation does not vary with height above the lake surface, and thus is not height corrected in the Lake Heat Flux Analyzer program.

2.2. Bulk parameterization of surface fluxes

The following section describes the algorithms used to estimate the surface energy fluxes from lake buoy data. The calculated surface heat fluxes (W m^{-2}) are: the reflected short-wave radiation (Q_{sr}), the sensible (Q_h) and latent (Q_e) heat fluxes, the incoming long-wave (Q_{lin}) and the outgoing long-wave radiation (Q_{lout}), expressed in terms of the total surface heat flux (Q_{tot}) as:

$$Q_{tot} = Q_{sin} + Q_{lin} - Q_{sr} - Q_e - Q_h - Q_{lout}, \qquad (1)$$

where Q_{sin} is the flux of short-wave radiation incident on the lake surface. To calculate these fluxes a variety of input variables are required: surface water temperature, air temperature, relative humidity, wind speed, and short-wave radiation. In addition, the measurement height of the sensors above the water surface is needed.

2.2.1. Incident and reflected short-wave radiation

The insolation (direct solar and diffuse sky radiation) reaching the lake surface is a large variable term in the heat budget of a lake and can be measured directly, using relatively inexpensive radiometers. Lake Heat Flux Analyzer does not compute short-wave radiation, but instead takes it as an input parameter. The reflected short-wave radiation, however, is rarely measured by instrumented lake buoys and must, therefore, be estimated from empirical relationships, the most common of which is in terms of the albedo, α_{sw}, as $Q_{sr} = \alpha_{sw} Q_{sin}$. Lake Heat Flux Analyzer calculates α_{sw} from Fresnel's Equation as:

$$\alpha_{sw} = \frac{1}{2}\left[\frac{(\sin^2 Z - R)}{(\sin^2 Z + R)} + \frac{(\tan^2 Z - R)}{(\tan^2 Z + R)}\right] \qquad (2)$$

where R is the angle of refraction, calculated from Snell's law as:

$$R = \sin^{-1}\left(\sin(Z)/\eta\right), \qquad (3)$$

where $\eta = 1.33$ is the index of refraction (Kirk, 1994) and Z is the solar zenith angle calculated as a function of latitude (φ), solar declination (δ) and the hour angle (H):

$$Z = \cos^{-1}\left(\sin\left(\frac{2\varphi\pi}{360}\right)\sin\left(\frac{2\delta\pi}{360}\right) + \cos\left(\frac{2\varphi\pi}{360}\right)\cos\left(\frac{2\delta\pi}{360}\right)\cos H\right), \quad (4)$$

$$\delta = \frac{180}{\pi}(0.006918 - 0.399912\cos(\gamma) + 0.070257\sin\gamma - 0.006758\cos 2\gamma$$

$$+ \, 0.000907\sin 2\gamma - 0.002697\cos 3\gamma + 0.00148\sin 3\gamma), \quad (5)$$

$$\gamma = 2\pi(DOY - 1)/365, \qquad (6)$$

$$H = (\pi/12)(t_{noon} - t), \qquad (7)$$

where DOY is the day of year (e.g. Jan 10 = 10), t_{noon} is the local solar noon and t is local solar time.

2.2.2. Net long-wave radiation

The net long-wave heat flux (Q_{lnet}) across the air-water interface comprises two main components: (i) incoming long-wave radiation (Q_{lin}) and (ii) outgoing long-wave radiation (Q_{lout}). The bulk formulae may be expressed as:

$$Q_{l_{net}} = Q_{lin} - Q_{lout}, \qquad (8)$$

where in the absence of direct measurements, we estimate these terms from frequently measured variables. In Lake Heat Flux Analyzer, incoming long-wave radiation, Q_{lin}, is estimated following the methods of Crawford and Duchon (1999), as:

$$Q_{lin} = \left\{clf + (1 - clf)\left(1.22 + 0.06\sin\left[(m+2)\frac{\pi}{6}\right]\right)\left(\frac{e_z}{T_{zK}}\right)^{1/7}\right\}\sigma T_{zK}{}^4, \quad (9)$$

where m is the numerical month (e.g. January = 1), T_{zK} is air temperature in Kelvin, e_z is the vapour pressure of the air (hPa) estimated based on the saturation vapour pressure of the air, and $\sigma = 5.67 \times 10^{-8}$ W m^{-2} K^{-4} is the Stefan-Boltzmann constant. The cloud cover fraction, clf, is estimated as $clf = 1 - s$, where s is the ratio of the measured short-wave radiation (i.e. Q_{sin}) to the estimated clear-sky short-wave radiation. Clear-sky short-wave radiation is estimated by Lake Heat Flux Analyzer following the methods of Meyers and Dale (1983) as shown in detail within the user manual of this program (see p.19 of the online user manual). However, as this calculation is based on the ratio of clear-sky and measured short-wave radiation, incoming long-wave radiation cannot be calculated at night. In this program, we estimate night-time incoming long-wave radiation based on the daytime averages of the cloud cover fraction. Therefore, the night-time incoming long-wave radiation is calculated as a function of air temperature, water vapour, and the daytime average cloud cover fraction. This adds an additional source of uncertainty in these estimates, but in comparison to other incoming long-wave formulae (e.g. Gill, 1982), which are daily averages, this method has been shown to provide a more accurate representation of incoming long-wave radiation (Crawford and Duchon, 1999).

Unlike the incoming long-wave radiation, which requires a number of input variables in its calculation, the outgoing long-wave radiation, Q_{lout}, is much less complicated to calculate. In Lake Heat Flux Analyzer, the outgoing long-wave radiation is estimated as a function of water temperature as:

$$Q_{l_{out}} = \varepsilon_w \sigma T_{0K}{}^4, \qquad\qquad (10)$$

where $\varepsilon_w = 0.972$ (Davies et al. 1971) is the emissivity of water and T_{0K} is the surface water temperature in Kelvin.

2.2.3. Bulk algorithms for momentum, sensible and latent heat fluxes

The turbulent heat fluxes, sensible heat and latent heat, are parameterized by bulk heat transfer algorithms that relate surface layer data to surface fluxes using formulae based on scaling laws and empirical relationships. The program uses a similar method to calculate, τ, the air-water momentum flux (N m^{-2}). These procedures involve the calculation of roughness lengths for momentum, heat and moisture (z_o, z_{oh}, z_{oq}) and the corresponding transfer coefficients (C_{d_z}, C_{h_z}, C_{e_z}) from observed wind speed (u), temperature (T) and humidity (q) profiles, via an iterative routine that involves a friction velocity term, u_{*a} (m s^{-1}), a scaling temperature term, T_* (K), and a scaling humidity term, q_* (g kg^{-1}). Using the above terms, surface fluxes for momentum, sensible heat and latent heat can be calculated as:

$$\tau = C_{d_z}\, \rho_z\, u_z^2 = \rho_z u_{*a}^2, \tag{11}$$

$$Q_h = \rho_z C_{pa} C_{h_z} u_z (T_0 - T_z) = -\rho_z C_{pa} u_{*a} T_*, \tag{12}$$

$$Q_e = \rho_z L_v C_{e_z} u_z (q_0 - q_z) = -\rho_z L_v u_{*a} q_*, \tag{13}$$

where $\rho_z = 100p/[R_a(T_z + 273.16)]$ is the density (kg m^{-3}) of the overlying air, p is the surface air pressure (hPa) and $R_a = 287(1 + 0.608 q_z)$ is the gas constant for moist air (J kg^{-1} °C^{-1}) ; u_z is the wind speed (m s^{-1}) at height z_u (m) above the water surface; $C_{pa} = 1006$ is the specific heat of air at constant pressure (J kg^{-1} °C^{-1}); T_0 is the surface water temperature (°C); T_z is air temperature (°C) at height z_t (m) above the water surface; $L_v = 2.501 \times 10^6 - 2370 \times T_0$ is the latent heat of vaporization (J kg^{-1}); $q_0 = \lambda e_{sat}/[p + (\lambda - 1)e_{sat}]$ is the specific humidity at saturation pressure (kg kg^{-1}), λ (= 0.622) is the ratio of the molecular weights for dry and moist air; e_{sat} is the saturated vapour pressure (hPa) calculated as $e_{sat} = 6.11 \exp[17.27 T_0 /(237.3 + T_0)]$; $q_z = \lambda e_z/[p + (\lambda - 1)e_z]$ is the specific humidity of the air (kg kg^{-1}) at height z_q (m) above the water surface, $e_z = R_h e_s/100$, R_h is the relative humidity (%) and $e_s = 6.11 \exp[17.27 T_z /(237.3 + T_z)]$ is the saturated vapour pressure (hPa) at z_t. Here, C_{d_z}, C_{h_z} and C_{e_z} are transfer coefficients for heights z_u, z_t and z_q, respectively.

A variety of bulk flux algorithms is presently used in the literature (e.g. Zeng et al. 1998; Fairall et al. 2003; Verburg and Antenucci, 2010). While these algorithms all use equations (11) to (13) to calculate the surface fluxes, they differ in the parameterization of the transfer coefficients, the treatment of free convective conditions and surface layer gustiness. Turbulent fluxes in the Lake Heat Flux Analyzer program were calculated following Zeng et al. (1998), which has been shown to be one of the least problematic bulk aerodynamic algorithms currently used by the scientific community (Brunke et al. 2003). This algorithm applies Monin-Obukhov similarity theory to the atmospheric boundary layer and states that wind, temperature and humidity profile gradients depend on unique functions of the stability parameter, ζ, where $\zeta = zL_w^{-1}$:

$$\phi_m(\zeta) = \frac{\kappa z_u}{u_{*a}}\frac{\partial u}{\partial z}, \tag{14}$$

$$\phi_h(\zeta) = \frac{\kappa z_t}{T_*}\frac{\partial T}{\partial z}, \tag{15}$$

$$\phi_e(\zeta) = \frac{\kappa z_q}{q_*}\frac{\partial q}{\partial z}, \tag{16}$$

where L_w is the Monin-Obukhov length scale (m), κ is the von Karman constant (= 0.41) and ϕ_m, ϕ_h and ϕ_e are the similarity functions that relate the fluxes of momentum, heat and moisture to the mean profile gradients of wind, temperature, and humidity, respectively. According to Brutsaert (1982), the Monin-Obukhov length scale is a measure of the ratio of the reduction of potential energy caused by wind mixing and the growth of atmospheric stratification due to surface fluxes and may be calculated following Monin and Obukhov (1954) as:

$$L_w = \frac{-\rho_z u_{*a}^3 T_v}{\kappa g\left(\frac{Q_h}{C_{pa}} + 0.61\frac{(T_z + 273.16)Q_e}{L_v}\right)}, \tag{17}$$

where $T_v = (T_z + 273.16)(1 + 0.61q_z)$ is the virtual air temperature (K) and $g = 9.780310[1 + 0.00530239 \sin^2\varphi - 0.00000587\sin^2 2\varphi - (31.55 \times 10^{-8}) \times h]$ is the gravitational acceleration (m s^{-2}) where φ is latitude (°) and h it altitude (m).

Following Zeng et al. (1998), the differential equations for ϕ_m, ϕ_h and ϕ_e can be integrated between the roughness length and measurement height, to obtain wind, temperature and humidity gradients in the atmospheric boundary layer and the corresponding scaling parameters used in calculating the turbulent surface fluxes. In addition, these are used to estimate wind speed, air temperature and humidity at any reference height (e.g. 10 m) above the lake surface (see user manual for full calculations). Using the Monin-Obukhov similarity theory, the flux gradient relations for momentum $(\phi_m(\zeta))$ are:

$$\phi_m(\zeta) = 5 + \zeta \qquad \text{for } \zeta > 1 \text{ (very stable)}, \qquad (18)$$

$$\phi_m(\zeta) = 1 + 5\zeta \qquad \text{for } 0 \leq \zeta \leq 1 \text{ (stable)}, \qquad (19)$$

$$\phi_m(\zeta) = (1 - 16\zeta)^{-1/4} \qquad \text{for } -1.574 \leq \zeta < 0 \text{ (unstable)}, \qquad (20)$$

$$\phi_m(\zeta) = (0.7\kappa^{2/3})(-\zeta)^{1/3} \qquad \text{for } \zeta < -1.574 \text{ (very unstable)}, \qquad (21)$$

and for sensible heat and humidity, where $\phi_e(\zeta) = \phi_h(\zeta)$, are:

$$\phi_h(\zeta) = \phi_e(\zeta) = 5 + \zeta \qquad \text{for } \zeta > 1 \text{ (very stable)}, \qquad (22)$$

$$\phi_h(\zeta) = \phi_e(\zeta) = 1 + 5\zeta \qquad \text{for } 0 \leq \zeta \leq 1 \text{ (stable)}, \qquad (23)$$

$$\phi_h(\zeta) = \phi_e(\zeta) = (1 - 16\zeta)^{-1/2} \qquad \text{for } -0.465 \leq \zeta < 0 \text{ (unstable)}, \qquad (24)$$

$$\phi_h(\zeta) = \phi_e(\zeta) = 0.9\kappa^{4/3}(-\zeta)^{-1/3} \qquad \text{for } \zeta < -0.465 \text{ (very unstable)}, \qquad (25)$$

where to ensure continuous functions of $\phi_m(\zeta)$, $\phi_h(\zeta)$ and $\phi_e(\zeta)$, we can match the relations at $\zeta_m = -1.574$ for $\phi_m(\zeta)$ and $\zeta_h = \zeta_e = -0.465$ for $\phi_h(\zeta) = \phi_e(\zeta)$. The flux gradient relations can then be integrated to yield profiles for wind, temperature and humidity, as well as the corresponding scaling terms. The scaling terms can then be used to calculate the surface fluxes for momentum, sensible heat and moisture as well as the corresponding

transfer coefficients as $C_{d_z} = u_{*a}{}^2/u_z{}^2$, $C_{h_z} = -u_{*a}T_*/u_z(T_0 - T_z)$ and $C_{e_z} = -u_{*a}q_*/u_z(q_0 - q_z)$, respectively.

By correcting for measurement height and the stability of the atmospheric boundary, we can also estimate the transfer coefficients at a standard height of 10 m as $C_{d10} = u_{*a}{}^2/u_{10}{}^2$, $C_{h10} = -u_{*a}T_*/u_{10}(T_0 - T_{10})$, and $C_{e10} = -u_{*a}q_*/u_{10}(q_0 - q_{10})$, respectively, where u_{10} is the wind speed at 10 m, T_{10} is air temperature at 10 m and q_{10} is the specific humidity at 10 m calculated following Zeng et al (1998), as explained in detail in the online user manual of this program. Once Q_e is known, evaporation rates may be calculated as $E = Q_e/\rho_0 L_v$, where $\rho_0 = 10^3 \times (1 - 1.9549 \times 10^{-5}|T_0 - 3.84|^{1.68})$ is the density (kg m^{-3}) of the surface water (Henderson-Sellers, 1986). A more detailed description of the methods used for calculating each output variable of this program is provided in the user manual.

2.3. Program structure

Lake Heat Flux Analyzer is structured in the same manner as Lake Analyzer (Read et al. 2011), which was developed for the GLEON, a grassroots organization centred on scientific collaboration and analysis of high-frequency lake buoy data. Similar to Lake Analyzer, data requirements (Table 1) for Lake Heat Flux Analyzer vary depending on the user-defined output selections (Table 2). This allows the program to be flexible with respect to data sources, instead of requiring all potential data files or functions for each program to be run. This structure not only increases program speed but also allows users with data limitations to use the program as some calculations require fewer inputs. For a more detailed description of the general program structure, see the user manual provided at heatfluxanalyzer.gleon.org.

Table 1. Input parameters to the Lake Heat Flux Analyzer program. Specific data format requirements are provided in the user manual.

Input	Units	Description
.wtr	°C	Tab delimited text file of surface water temperature measurements.
.wnd	m s^{-1}	Tab delimited text file of wind speed measurements.
.airT	°C	Tab delimited text file of air temperature measurements.
.rh	%	Tab delimited text file of relative humidity measurements.
.sw	W m^{-2}	Tab delimited text file of short-wave radiation measurements.
.lwnet	W m^{-2}	Tab delimited text file of net long-wave radiation measurements.
.lw	W m^{-2}	Tab delimited text file of incoming long-wave radiation measurements.
.par	mmol m^{-2} s^{-1}	Tab delimited text file of photosynthetically active radiation measurements. This file is only used when a .sw file is missing.
z_u	m	Height of wind measurement.
z_q	m	Height of relative humidity measurement.
z_t	m	Height of air temperature measurement.
Output resolution	s	Output resolution of results.
h	m	Altitude of lake.
φ	°	Latitude of lake (positive for Northern Hemisphere and negative for Southern Hemisphere).
Max wind speed	m s^{-1}	Maximum wind speed allowed.
Min wind speed	m s^{-1}	Minimum wind speed allowed.

Table 2. Output variables from the Lake Heat Flux Analyzer program including a list of input files required for the corresponding outputs.

Output	Units	Description	Surface water temperature (.wtr)	Wind speed (.wnd)	Air temperature (.airT)	Relative humidity (.rh)	Short-wave radiation (.sw)	Additional parameters
u_{*a}	m s⁻¹	Air friction velocity	✓	✓	✓	✓		z_u, z_t, z_q, alt
u_{*aN}	m s⁻¹	Air friction velocity (neutral)		✓				z_u
T_{10}	°C	Air temperature at 10 m	✓	✓	✓	✓		z_u, z_t, z_q, alt
E	mm day⁻¹	Evaporation	✓	✓	✓	✓		z_u, z_t, z_q, alt
Q_{lin}	W m⁻²	Incoming long-wave radiation			✓	✓	✓	φ
Q_e	W m⁻²	Latent heat flux	✓	✓	✓	✓		z_u, z_t, z_q, alt
τ	N m⁻²	Momentum flux	✓	✓	✓	✓		z_u, z_t, z_q, alt
L_w	m	Monin-Obukhov length scale	✓	✓	✓	✓		z_u, z_t, z_q, alt
Q_{lnet}	W m⁻²	Net long-wave radiation	✓		✓	✓	✓	alt, φ
Q_{lout}	W m⁻²	Outgoing long-wave radiation	✓					
Q_{sr}	W m⁻²	Reflected short-wave radiation					✓	φ
rh_{10}	%	Relative humidity at 10 m	✓	✓	✓	✓		z_u, z_t, z_q, alt
Q_h	W m⁻²	Sensible heat flux	✓	✓	✓	✓		z_u, z_t, z_q , alt
C_h	-	Transfer coefficient for heat	✓	✓	✓	✓		z_u, z_t, z_q, alt
C_{hN}	-	Transfer coefficient for heat (neutral)		✓				z_u
C_{h10}	-	Transfer coefficient for heat at 10 m	✓	✓	✓	✓		z_u, z_t, z_q, alt
C_{hN10}	-	Transfer coefficient for heat at 10 m (neutral)		✓				z_u
C_e	-	Transfer coefficient for humidity	✓	✓	✓	✓		z_u, z_t, z_q, alt
C_{eN}	-	Transfer coefficient for humidity (neutral)		✓				z_u
C_{e10}	-	Transfer coefficient for humidity at 10 m	✓	✓	✓	✓		z_u, z_t, z_q, alt
C_{eN10}	-	Transfer coefficient for humidity at 10 m (neutral)		✓				z_u, z_t, z_q, alt

C_d	-	Transfer coefficient for momentum	✓	✓	✓	✓		z_u, z_t, z_q, alt
C_{dN}	-	Transfer coefficient for momentum (neutral)		✓				z_u
C_{d10}	-	Transfer coefficient for momentum at 10 m	✓	✓	✓	✓		z_u, z_t, z_q, alt
C_{dN10}	-	Transfer coefficient for momentum at 10 m (neutral)		✓				z_u
u_{10}	m s^{-1}	Wind speed at 10 m	✓	✓	✓	✓		z_u, z_t, z_q, alt
u_{10N}	m s^{-1}	Wind speed at 10 m (neutral)		✓				z_u

3. Results

The following section demonstrates applications of the Lake Heat Flux Analyzer program using examples with some of the different time periods and average times available to the user. Observed daily averaged incoming long-wave radiation measurements for Lake Mendota compare well ($r^2 = 0.74$, p < 0.001) with those estimated by the Lake Heat Flux Analyzer program (Fig. 1). For the time period shown, the seasonal patterns for the observed and estimated incoming long-wave radiation were very similar, varying by less than 20 W m^{-2} over the investigation period. Clear seasonal patterns were also evident for the outgoing long-wave radiation, which on average was 56.2 W m^{-2} greater than the estimated incoming long-wave radiation throughout the year.
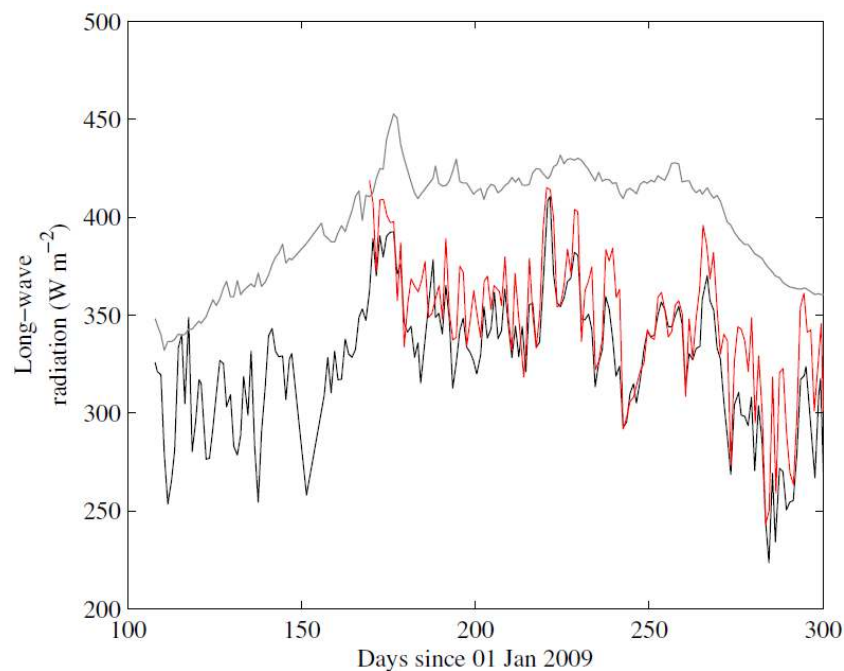
Figure 1. Daily-averaged calculated (black) and modelled (red) incoming and outgoing (grey) long-wave radiation for Lake Mendota in 2009.

For a seven-day period during summer at Esthwaite Water, the hourly averaged wind speed varied from < 1 to 8 m s^{-1}. Differences between measured wind speed at the lake surface (2.85 m) and those estimated at a height of 10 m (i.e. estimated by Lake Heat Flux

Analyzer) were variable throughout the study period (Fig. 2a). On day of year 301, for example, the estimated wind speed at 10 m was approximately 40% greater than that measured at the lake surface. During low-wind conditions the stability parameter ($z_u L_w^{-1}$) was negative (Fig. 2b), often reaching the lower threshold of -15 which is commonly used as a cutoff during the computation of the stability parameter (e.g. Imberger and Patterson, 1990; MacIntyre et al. 2002), and the drag coefficient was high (Fig. 2c). Furthermore, as the stability parameter approached zero, the drag coefficients calculated at 10 m closely matched those calculated at the measurement height. When the stability parameter approached zero during high winds, the transfer coefficient was generally low. The need to calculate transfer coefficients accurately at high-resolution is illustrated by the large changes evident in the drag coefficient, varying by over an order of magnitude within the 24-hour period. When the atmosphere was stable ($z_u L_w^{-1} > 0$), C_{d10} was lower than C_{d_z} and when the atmosphere was unstable ($z_u L_w^{-1} < 0$), estimates of C_{d10} were higher than C_{d_z}. The momentum flux, τ, also varied by an order of magnitude, closely following the change in wind speed, where a sharp increase or decrease in wind speed was reflected in an increase or decrease in the momentum flux (Fig. 2d).
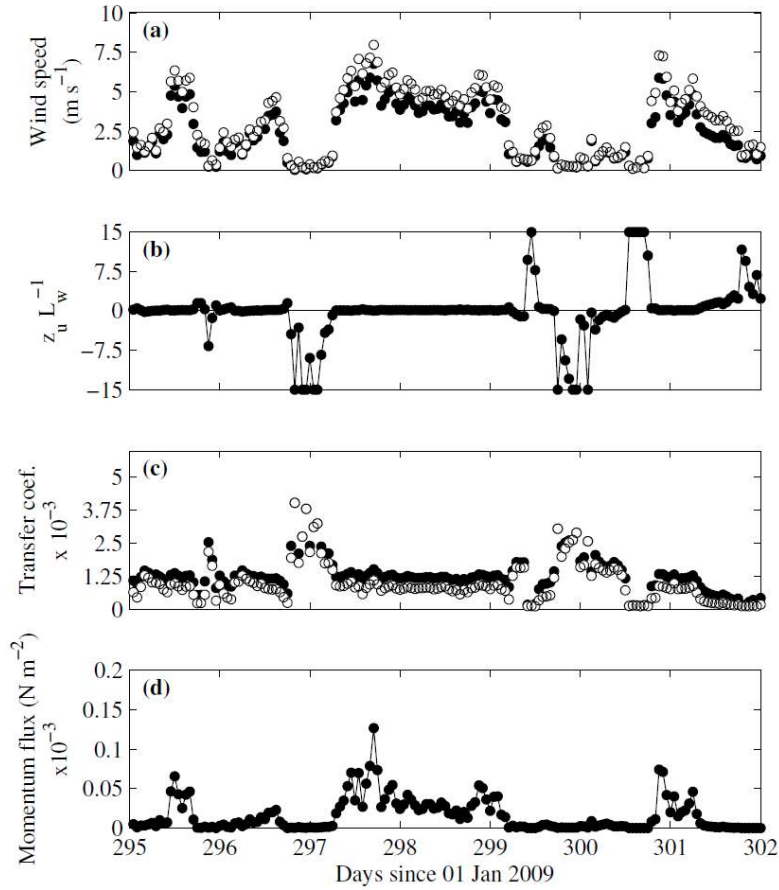
Figure 2. High-frequency (hourly) measurements for seven days during the stratified period in Esthwaite Water of (a) wind speed measured at the sensor height (closed circles) and calculated at a height of 10 m (open circles); (b) atmospheric stability parameter, $z_u L_w^{-1}$, bounded by ±15; (c) transfer coefficient for momentum at the sensor height (closed circles) and calculated at a height of 10 m (open circles); (d) shear stress (i.e. momentum flux) at the water surface.

In Rotorua, an example 24-hour period during spring (Fig. 3) highlights the variability in air temperature at high temporal resolution as well as the variability with height above the water surface (Fig. 3a). When the atmospheric boundary layer was stable, which can be determined by the difference between air and surface water temperatures (Croley, 1989; Derecki, 1981), air temperature calculated at 10 m was marginally higher than that measured at the sensor height. However, when the atmospheric boundary layer was unstable, air temperature at the measurement height was greater than that at 10 m. As expected, the

20

transfer coefficient for sensible heat at the measurement height was consistently higher than that at 10 m (Fig. 3b) and the difference between the transfer coefficients at these heights was greater when the atmosphere was unstable. Similar to the transfer coefficient for momentum, the transfer coefficient for heat varied substantially over a 24-hour period. There was also a large hourly variation in the sensible heat flux (Fig. 3c), including a change in the direction of heat flux (i.e. heating/cooling), despite the minimal change in lake surface water temperature.
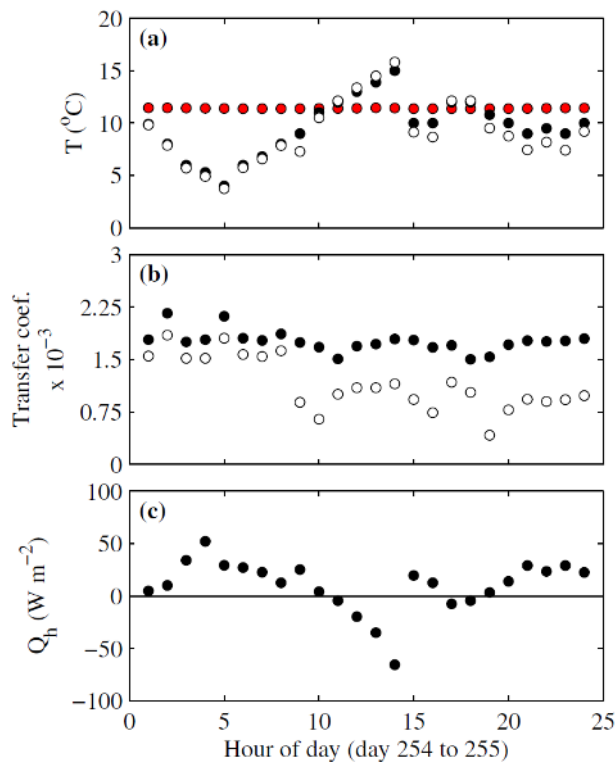
Figure 3. High-frequency (hourly) measurements for a 24-hour period in Rotorua during spring, showing (a) air temperature measured at the sensor height (closed circles), air temperature estimated at height of 10 m (open circles) and water temperature (red); (b) transfer coefficient for sensible heat estimated at the sensor height (closed circles) and estimated at 10 m (open circles); (c) sensible heat flux.

Incoming short-wave radiation was a large contributor to the total daily surface heat flux in Esthwaite Water during the stratified period (Fig. 4a), often being up to three times

larger than the net long-wave radiation, which is generally a cooling term, and an order of magnitude larger than the reflected short-wave radiation. Of the surface turbulent fluxes (Fig. 4b), the latent heat flux is the largest contributor to the total surface heat flux, being twice that of the sensible heat flux for the selected period. Both latent and sensible heat fluxes are generally cooling fluxes, but both can also provide heating. The latent heat flux, for example, can provide heating during dew formation.
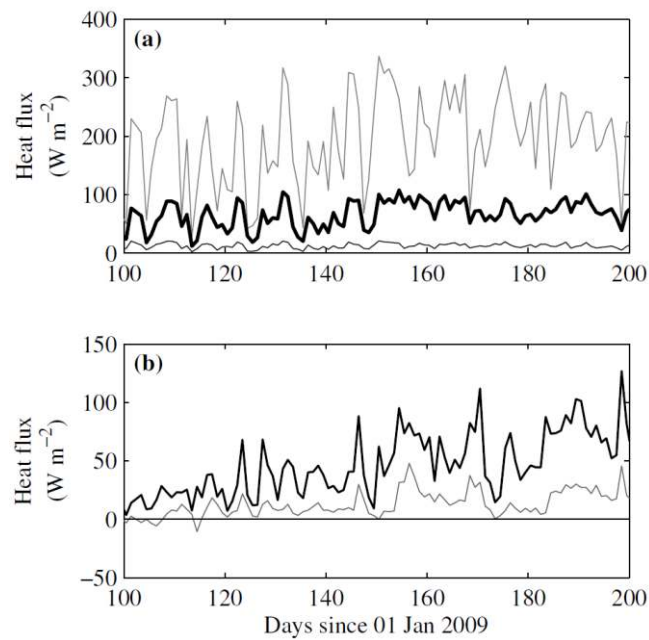
Figure 4. Time series of calculated daily averages of (a) incoming (grey) and reflected (thin black) short-wave radiation, and net long-wave radiation (thick line); (b) latent (black) and sensible (grey) heat flux for Esthwaite Water in 2009.

Lake Heat Flux Analyzer can calculate the surface fluxes for many lakes in a consistent way, allowing a robust comparison among sites. For the three example lakes shown here, the daily averaged total surface heat flux (Fig. 5) varied considerably. As expected, Q_{tot} was predominantly positive (i.e. heat entering the lake) during the period shown. All three lakes demonstrated a seasonal pattern in Q_{tot}, although Lake Mendota experienced the greatest magnitude throughout the period shown. Daily averaged data are

often not ideal for comparison. However, longer averages can also be obtained from the Lake

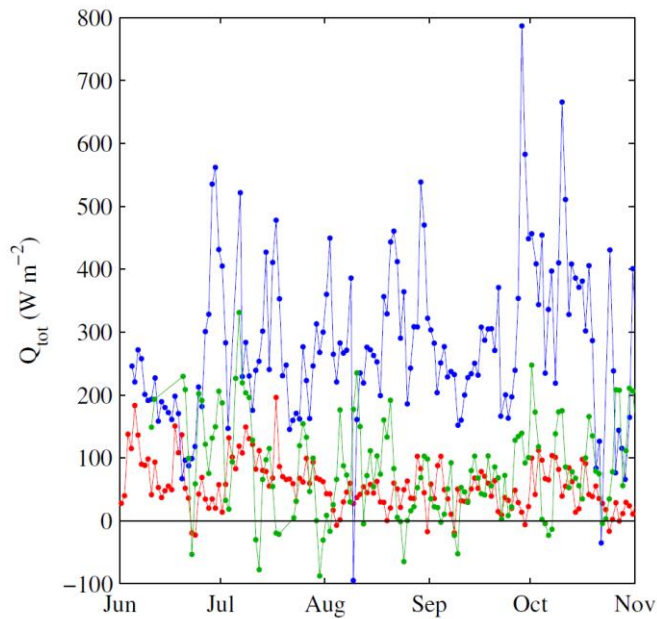Heat Flux Analyzer program to illustrate better the difference among sites

Figure 5. Time series of the calculated daily averages of total surface energy fluxes, Q_{tot}, for Esthwaite Water (red), Lake Mendota (blue) and Rotorua (green).

Lake Heat Flux Analyzer can also be used to calculate evaporation rates. Monthly averaged evaporation rates were lowest for Esthwaite Water and highest for Lake Mendota during the specified months (Fig. 6). Seasonal patterns in the evaporation rates occur and were largest in summer and smallest in winter for these lakes. For the Northern Hemisphere lakes, evaporation rates for Lake Mendota were considerably higher than for Esthwaite Water, on occasion being five times as large. For Rotorua, evaporation rates were lowest in July, which corresponds to winter, and highest in November, corresponding to late spring.
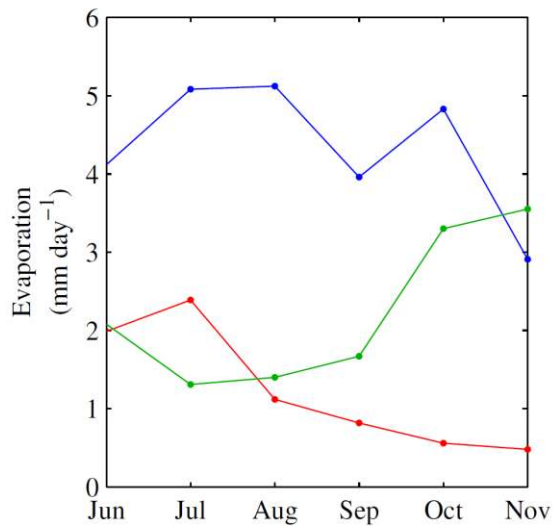
Figure 6. Calculated monthly-averaged evaporation rates for Esthwaite Water (red), Lake Mendota (blue) and Rotorua (green).

4. Discussion

Radiant and turbulent surface energy fluxes play an integral role in the functioning of lakes. These surface fluxes not only drive physical processes within a lake, but also affect the exchange of greenhouse gases. Quantifying these physical processes is therefore central to understanding lake dynamics and their contribution to global biogeochemical cycles. In recent years, the development of virtual networks of scientists has increased the ability to share ideas, hypotheses, data and methods. This has particular advantages for lake science as lakes are often characterized by high spatial and temporal variability (Kratz et al. 2003) and coupled physical/biological processes (Hamilton and Schladow, 1997). Recent developments in aquatic sensor technology have made it possible to monitor conditions in lakes remotely from *in situ* platforms (Hamilton et al. 2014). Many such platforms have been deployed worldwide and many lake stations are integrated into networks such as the GLEON and the Networking Lake Observatories in Europe (NETLAKE; https://www.dkit.ie/netlake). Many of these lake stations measure the variables needed to calculate surface energy fluxes. The software outlined here has been produced to exploit these data by creating a set of procedures for calculating the surface energy fluxes from lakes. They have been collated into an open source program called "Lake Heat Flux Analyzer" aimed at communities such as GLEON and NETLAKE, which are centred on scientific collaboration to further the understanding and management of lakes.

In the development of Lake Heat Flux Analyzer we aimed to overcome the difficulty of comparing surface flux estimates from various sites by using a consistent calculation procedure. In particular, we were motivated to understand how the individual terms of the surface energy budget vary across a diverse range of lakes. Several studies have suggested a number of factors that influence the turbulent surface fluxes in lakes, in particular, wind speed and atmospheric stability (e.g. Verburg and Antenucci, 2010). Higher wind speeds, for

example, increase wave height and therefore roughness length, which in turn acts to increase the drag coefficient (Brutsaert, 1982). At low wind speeds, however, waves cease to be the most important interface between the water and air, and other transfer mechanisms control the value of the transfer coefficients (Chang and Grossman, 1999). As seen in Figure 2, atmospheric stability can cause large variations in the transfer coefficients as the more stable the atmosphere the more restricted is the mixing from higher levels towards the air-water interface (Deardorff, 1968). As heat loss is enhanced when the atmospheric boundary layer is unstable (Fig. 3), a condition which can persist for long periods (Rouse et al. 2003), the latent and sensible heating terms can contribute substantially to the surface energy budget. Actual estimates of the transfer coefficient vary enormously in the literature (Garratt, 1992), where an order of magnitude increase between values in stable low wind speed conditions and those in unstable high wind conditions are often reported. As shown here, estimates of transfer coefficients can also vary at sub-daily timescales, owing to the difference in atmospheric stability and wind speed.

Since the pioneering work of Birge (1916), many studies have analyzed heat fluxes from lakes from around the world, including temperate lakes (Hutchinson and Edmondson, 1957), tropical lakes (Lewis, 1973), and subarctic lakes (Edmundson and Mazumder, 2002). A majority of the research, however, has been conducted on relatively long time scales, concentrating on the seasonal and intra-seasonal variation in the surface heating terms (e.g. Lenters et al. 2005), although some studies at higher temporal resolution do exist (e.g. Frempong, 1983; MacIntyre et al. 2002). For the lakes studied here, the surface energy fluxes varied considerably at both diel and seasonal time scales. In Esthwaite Water, for example, the exchange of radiant energy was dominated by short-wave radiation, being a larger contributor to the total surface heat flux than net long-wave radiation as well as the turbulent fluxes of latent and sensible heat. Program outputs demonstrated the variability in surface

heating/cooling within and among the three example lakes. The most evident difference among the lakes was in the evaporative heat flux, where during the same months, evaporation rates for Lake Mendota were more than double those of Esthwaite Water.

For a given lake we have confirmed that the transfer coefficients for momentum and sensible heat can vary substantially from the measurement height to a reference height of 10 m. Failing to consider the substantial difference in the estimated transfer coefficient based on wind speed measurements at different heights can lead to erroneous conclusions about the turbulent surface fluxes. We recommend that comparisons of transfer coefficients among sites should, therefore, be based on values corrected to 10 m and this program allows this correction to be made.

The methods outlined here have been used to generate a set of tools for calculating the surface energy fluxes from instrumented lake buoy data, which can be applied to lakes from around the world in a standardized way. The surface energy fluxes can be calculated rapidly by the Lake Heat Flux Analyzer program and provide a much-needed tool for the expanding global network of instrumented lakes. The limnological community has already benefitted from data analysis tools such as wavelet analysis (Torrence and Compo, 1998) and Lake Analyzer (Read et al. 2011) that have been used in global scale research (e.g. Winder and Cloern, 2010; Read et al. 2012). Similarly, Lake Heat Flux Analyzer can be used for global scale research by calculating the surface fluxes using the same method, which is essential for cross-site collaboration.

The algorithms presented were created for the rapid calculation of the surface energy fluxes from instrumented lake buoy data. The accuracy of the results, however, will depend upon the quality of the input data. The program does not include quality control procedures and assumes that instrument calibration has been performed. The algorithms also assume that the input data is measured on the lake, particularly wind speed, which will vary from that

measured on land (Markfort et al. 2010) and will have a substantial influence on the turbulent surface fluxes. A wind-sheltering coefficient is often applied to land-based wind measurements in numerical models to account for the difference in roughness lengths between land and open water (Brutsaert, 1982). If a sheltering coefficient is used prior to running Lake Heat Flux Analyzer, the results should be interpreted with caution.

Future demands for more accurate modelling approaches will require a more detailed simulation of surface fluxes. For example, Lake Heat Flux Analyzer may be used by analytical and numerical models to include additional processes, such as gas fluxes, and may also provide a rapid means to improve the fit of numerical models (Hamilton et al. 2014). Furthermore, the parameterizations currently used to estimate transfer coefficients are derived from the ocean and therefore may not cover all of the difficulties associated with lakes of varying size (Vachon and Prairie, 2013). Small lakes, for example, are often characterized by low wind speeds, potentially extreme stabilities, waves that have not attained equilibrium with forcing conditions and sufficiently shallow depths to compromise wave shape (Wüest and Lorke, 2003). The transfer coefficients have been described to be influenced by wave-age, where younger waves are considered more effective at transferring momentum at the air-water interface, with wave-age itself being implicitly related to wind speed and fetch (e.g. Donelan et al. 1993). Only when the wave-state reaches equilibrium with the atmosphere is the efficiency of transfer reduced to open ocean values. By using the transfer coefficients calculated from the open ocean, even when taking atmospheric stability and wind speed into account, limnologists are in danger of severely underestimating the turbulent fluxes across the air-water interface. In the future we should derive new transfer coefficients for lakes which may account for variation caused by, for example, sheltering and fetch-limitation of wind. With this in mind, we have written the numerical code in an easily accessible manner,

so that when new approaches are developed, they can be easily incorporated into the program.

5. Conclusions

We present a program called "Lake Heat Flux Analyzer" for calculating the surface energy fluxes using high-frequency data from instrumented lake buoys. The algorithms account for site specific features such as wind, temperature and humidity measurement height. The program was developed in MATLAB but can also be used via the online interface which only requires the input files for analysis. The program provides a powerful tool for comparative analysis of surface fluxes based on algorithms developed for individual components of the heat flux. The availability of this program will facilitate inter-lake analysis and lends itself to comparative studies of heat fluxes in lakes across the globe.

Acknowledgements

References

Anderson, W.L., Robertson, D.M., and Magnuson, J.J. 1996. Evidence of recent warming and El Nino-related variations in ice breakup of Wisconsin lakes. Limnol. Oceanogr. 41, 815-821.

Birge, E.A. 1916. The work of the wind in warming a lake. T. Wisc. Acad. Sci. 18, 341-391.

Blanc, T. V. 1985. Variation of bulk-derived surface flux, stability, and roughness results due to the use of different transfer coefficient schemes. J. Phys. Oceanogr. 15, 650-669.

Brunke, M.A., Fairall, C.W., Zeng, X., Eymard, L., and Curry, J. 2003. Which bulk aerodynamic algorithms are least problematic in computing ocean turbulent fluxes? J. Climate 16, 619-635.

Brutsaert, W.H. 1982. Evaporation into the atmosphere: Theory, history, and application. D. Riedel.

Chang, H., and Grossman, R. L. 1999. Evaluation of bulk surface flux algorithms for light wind conditions using data from the Coupled Ocean-Atmosphere Response Experiment (COARE). Quart. J. Roy. Meteor. Soc. 125, 1551-1588.

Crawford, T.M., and Duchon, C.E. 1999. An improved parameterization for estimating effective atmospheric emissivity for use in calculating daytime downwelling longwave radiation. J. Appl. Meteor., 38, 474-480.

Croley, T.E. 1989. Verifiable evaporation modeling on the Laurentian Great Lakes. Water Resour. Res. 25, 781-792.

Davies, J.A., Robinson, P.J., and Nunez, M. 1971. Field determinations of surface emissivity and temperature foe Lake Ontario. J. Appl. Meteorol. 10, 811-819.

De Stasio, B.T. Jr., Hill, D.K., Kleinhans J.M., Nibbelink N.P., and Maguson J.J. 1996. Potential effects of global climate change on small north-temperate lakes: Physics, fish and plankton. Limnol. Oceanogr. 41, 1136–1149.

Deardorff, J.W. 1968. Dependence of air-sea transfer coefficients on bulk stability. J. Geophys. Res. 73, 2549-2557.

Derecki, J.A. 1981. Stability effects on Great Lakes Evaporation. J. Great Lakes Res. 7, 357-362.

Desai, A.R., Austin, J.A., Bennington, V., McKinley, G.A. 2009. Stronger winds over a large lake in response to weakening air-to-lake temperature gradient. Nature Geosci. 2, 855-858.

Donelan, M.A., Dobson, F.W., Smith, S.D., and Anderson, R.J. 1993. On the dependence of sea surface roughness on wave development. J. Phys. Oceanogr. 23, 2143-2149.

Edmundson, J.A., and Mazumder, A. 2002. Regional and hierarchial perspectives of thermal regimes in subarctic, Alaskan lakes. Freshwater Biol. 47, 1-17.

Fairall, C.W., Bradley, E.F., Hare, J.E., Grachev, AA., Edson. 2003. Bulk parameterization of air-sea fluxes: updates and verification for the COARE algorithm. J. Climate 16: 571-591.

Fairall, C.W., Bradley, E.F., Rogers, D.P., Edson, J.B., Young, G.S. 1996. Bulk parameterization of air-sea fluxes for Tropical Ocean-Global Atmosphere Coupled-Ocean Atmosphere Response Experiment. J. Geophys. Res. Oceans. 101, 3747-3764.

Frempong, E. 1983. Diel aspects of the thermal structure and energy budget of a small English Lake. Freshwater Biol. 13, 89-102.

Garratt, J. R. 1977. Review of Drag Coefficients over Oceans and Continents. Mon. Weather Rev. 105, 915–929.

Garratt, J. R. 1992. The atmosphere boundary layer. Cambridge Atmospheric and Space Science Series. Cambridge University Press.

George, D.G., and Taylor, A.H. 1995. UK lake plankton and the Gulf Stream. Nature. 378, 139.

Gill, A.E. 1982. Atmosphere-ocean dynamics. International Geophysics Series, 30. Academic Press.

Hamilton, D.P., and Schladow, S.G. 1997. Prediction of water quality in lakes and reservoirs. Part 1 - Model description. Ecol. model. 96, 91-110.

Hamilton, D.P., Carey, C.C., Arvola, L., Arzberger, P., Brewer, C., Cole, J.J., Gaiser, E., Hanson, P.C., Ilbeings, B.W., Jennings, E., Kratz, T.K., Lin, F., McBride, C.G., Marques, D., Muraoka, K., Nishri, A., Qin, B., Read, J.S., Rose, K.C., Ryder, E., Weather, K.C., Zhu, G., Trolle, D., Brookes, J.D. 2014. A Global Lake Ecological Observatory Network (GLEON) for synthesising high-frequency sensor data for validation of deterministic ecological models. Inland waters 5, 49-56.

Hanson, P.C. 2007. A grassroots approach to sensor and science networks. Front. Ecol. Environ. 5, 343.

Henderson-Sellers, B. 1986. Calculating the surface energy balance for lake and reservoir modelling: A review. Rev. Geophys., 24, 625-649.

Hutchinson, G., and Edmondson, Y. 1957. A Treatise on limnology. Wiley.

Imberger, J., and Patterson, J.C. 1990. Physical Limnology. Adv. Appl. Mech. 27, 303-475.

Jones, I., George, G., Reynolds, C. 2005. Quantifying effects of phytoplankton on the heat budgets of two large limnetic enclosures. Freshwater Biol. 50: 1239-1247.

Kirk, J.T.O. 1994. Light and photosynthesis in aquatic ecosystems, 2 Ed., 528 Pp., Cambridge University Press.

Kratz, T.K., Deegan, L.A., Harmon, M.E., Lauenroth, W.K. 2003. Ecological variability in space and time: Insights gained from the US LTER program. Bioscience. 53, 57-67.

Large, W.G., and Pond, S. 1982. Sensible and latent heat flux measurements over the ocean. J. Phys. Oceanogr. 12, 464-482.

Lenters, J., Kratz, T., and Bowser, C. 2005. Effects of climate Variability on lake evaporation: Results from a long-term energy budget study of Sparkling Lake, northern Wisconsin (USA). J. Hydrol. 308, 168-195.

Lewis, W. 1973. Thermal regime of Lake Lanao (Philippines) and its theoretical implications for tropical lakes. Limnol. Oceanogr. 18, 200-217.

MacIntyre, S. 1993. Vertical mixing in a shallow, eutrophic lake: Possible consequences for the light climate of phytoplankton. Limnol. Oceanogr. 38,798:817.

MacIntyre, S., Jonsson, A., Jansson, M., Aberg, J., Turney, D.E., and Miller, S.D., 2010. Buoyancy flux, turbulence, and the gas transfer coefficient in a stratified lake. Geophys. Res. Lett. 37, doi: 10.1029/2010GL044164.

MacIntyre, S., Romero, J.R., and Kling, G.W. 2002. Spatial-temporal variability in surface layer deepening and lateral advection in an embayment of Lake Victoria, East Africa. Limnol. Oceanogr. 47, 656-671.

Mackay, E.B., Jones, I.D., Thackeray, S.J., and Folkard, A.M. 2011. Spatial heterogeneity in a small, temperate lake during archetypal weak forcing conditions. Fundam. Appl. Limnol. 179, 27-40.

Markfort, C.D., Perez, A.L.S., Thill, J.W., Jaster, D.A., Porté-Agel, F., and Stefan, H.G. 2010. Wind sheltering of a lake by a tree canopy or bluff topography. Water Resour. Res. 46, doi: 10.1029/2009WR007759.

Meyers, T.P., Dale, R.F. 1983. Predicting daily insolation with hourly cloud height and coverage. J. Clim. Appl. Meteorol. 22, 537-545.

Mitchell, K.E., Lohmann, D., Houser, P.R., Wood, E.F., Schaake, J.C., Robock, A., Cosgrove, B.A., Sheffield, J., Duan, Q., Luo, L., Higgins, R.W., Pinker, R.T., Tarpley, J.D., Lettenmaier, D.P., Marshall, C.H., Entin, J.K., Pan, M., Shi, W., Koren, V., Meng, J., Ramsay, B.H., and Bailey, A.A. 2004. The multi-institution North Americal Land Data Assimilation System (NLDAS): Utilizing multiple GCIP products and partners in a continental distributed hydrological modelling system. J. Geophys. Res. 109, doi: 10.1029/2003JD003823.

Monin, A.S., and Obukhov, A.M. 1954. Basic laws of turbulent mixing in the atmosphere near the ground, J.Akad. Nauk. SSR. Geofiz. Inst., 24, 163-187.

Peeters, F., Livingstone, D.M., Goudsmit, G., Kipfer, R., and Forster, R. 2002. Modeling 50 years of historical temperature profiles in a large central European lake. Limnol. Oceanogr. 47, 186-197.

Porter, J.H., Hanson, P.C., and Lin, C. 2012. Staying afloat in the sensor data deluge. Trends Ecol. Evol. 27, 121-129.

Read, J.S., Hamilton, D.P., Desai, A.R., Rose, K.C., MacIntyre, S., Lenters, J.D., Smyth, R.L., Hanson, P.C., Cole, J.J., Staehr, P.A., Rusak, J.A., Pierson, D.C., Brookes, J.D., Laas, A., and Wu, C.H. 2012. Lake-size dependency of wind shear and convection as controls on gas exchange. Geophys. Res. Lett. 39, doi: 10.1029/2012GL051886.

Read, J.S., Hamilton, D.P., Jones, I.D., Muraoka, K., Winslow, L.A., Kroiss, R., Wu, C.H., and Gaiser, E. 2011. Derivation of lake mixing and stratification indices from high-resolution lake buoy data. Environ. Modell. Softw. 26, 1325-1336.

Renfrew, I. A., Moore, G.W.K., Guest, P.S., Bumke, K. 2002. A comparison of surface layer and surface turbulent flux observations over the Labrador Sea with ECMWF analyses and NCEP reanalyses. J. Phys. Oceanogr. 32, 383-400.

Rouse, W.R., Oswald, C.M., Binyamin, J., Blanken, P.D., Schertzer, W.M., and Spence, C. 2003. Interannual and seasonal variability of the surface energy balance and temperature of central Great Lake Slave. J. Hydrometeorol. 4, 720-730.

Solomon, C.T., Bruesewitz, D.A., Richardson, D.C., Rose, K.C., Van de Bogert, M.C., Hanson, P.C., Kratz, T.K., Larger, B., Adrian, R., Babin, B.L., Chiu, C., Hamilton, D.P., Gaiser, E., Hendricks, S., Istvánovics, V., Lass, A., O'Donnell, D.M., Pace, M.L., Ryder, E., Staehr, P.A., Torgersen, T., Vanni, M.J., Weathers, K.C., Zhu, G. 2013. Ecosystem respiration: Drivers of daily variability and background respiration in lakes around the globe. Limnol. Oceanogr. 58, 849-866.

Staehr, P.A., Bade, D., Van de Bogert, M.C., Koch, G.R., Williamson, C., Hanson, P.C., Cole, J.J., Kratz, T. 2010. Lake metabolism and the diel oxygen technique: state of the science. Limnol. Oceanogr. Methods. 8: 628-644.

Strub, P.T., and Powell, T. 1986. Wind-driven surface transport in stratified closed basins: direct versus residual calculation. J. Geophys. Res. 91, 8497-8508, doi: 10.1029/JC091iC07p08497.

Torrence, C., and Compo, G.P. 1998. A practical guide to wavelet analysis. B. Am. Meteorol. Soc. 79, 61-78.

Vachon, D., and Prairie, Y.T. 2013. The ecosystem size and shape dependence of gas transfer velocity versus wind speed relationship in lakes. Can. J. Fish. Aquat. Sci. 70, 1757-1764.

Verburg, P., and Antenucci, J.P. 2010. Persistent unstable atmospheric boundary enhances sensible and latent heat loss in a tropical great lake: Lake Tanganyika. J. Geophys. Res. 115, doi: 10.1029/2009JD012839.

Wetzel, R.G., and Likens G.E. 1991. The heat budget of lakes. Limnological Analyses. Springer New York, 43-53

Winder, M., and Cloern, J.E. 2010. The annual cycles of phytoplankton biomass. Philos. T. Roy. Soc. B. 365, 3215-3226.

Winder, M., and Schindler, D.E. 2004. Climate effects on the phenology of lake processes. Glob. Change Biol. 10: 1844-1856.

Wüest, A., and Lorke, A. 2003. Small-scale hydrodynamics in lakes. Annu. Rev. Fluid. Mech. 35: 373-412.

Zeng, X., Zhao, M., and Dickinson, R.E. 1998. Intercomparison of bulk aerodynamic algorithms for the computation of sea surface fluxes using TOGA COARE and TAO data. J. Climate. 11, 2628-264